ACS OMEGA

http://pubs.acs.org/journal/acsodf

Article

Geochemistry and Organic Petrology of Middle Permian Source Rocks in Taibei Sag, Turpan-Hami Basin, China: Implication for Organic Matter Enrichment

Huan Miao,* Yanbin Wang, Shihu Zhao, Jianying Guo,* Xiaoming Ni, Xun Gong, Yujian Zhang, and Jianhong Li

Cite This: *ACS Omega* 2021, 6, 31578−31594

Read Online

ACCESS | Metrics & More | Article Recommendations

ABSTRACT: The Taodonggou group of Middle Permian is an important source rock in Taibei sag of Turpan-Hami basin. Due to its deep burial, drilling has only been revealed in recent years. Based on organic petrology and organic geochemistry experiments, this paper studies the organic petrology, organic geochemistry, sedimentary environment, and hydrocarbon generation potential of source rocks in Taibei sag, Turpan-Hami basin, and reveals the influence of the sedimentary environment on the organic matter abundance of source rocks. The results are as follows: (1) The organic matter of the Middle Permian source rocks in Taibei sag of Turpan-Hami basin is mainly sapropelite and exinite. The vitrinite is mainly vitrodetrinite, and the exinite is mainly lamalginiite. (2) The total organic carbon content value is 0.55−6.08 wt %, and the average value is 2.58 wt %. The PG value ranges from 0.78 mg HC/g to 30.86 mg HC/g, and the average value is 4.88 mg HC/g. Chloroform asphalt "A" is 0.046−0.8767 wt %, and the average value is 0.285 wt %. The types of organic matter are mainly III and II−III, and the R_o value is 0.628−1.49 wt % (average = 0.988 wt %). The T_{max} distribution is 329−465 °C. The average temperature is 434.7 °C, which is in the mature stage (oil window stage). The Middle Permian source rocks are mainly very good to excellent source rocks with a good hydrocarbon generation potential. (3) The source rocks are deposited in a semihumid and semiarid climate. Organic matter is input as a mixed source. The early and late stages is dominated by terrestrial higher plants. The middle stage is dominated by lower aquatic organisms, and the sedimentary environment consists of weak reduction and weak oxidation environments. (4) In the study area, the abundance of organic matter has a weak negative correlation with CPI and a positive correlation with Pr/Ph and $\sum C_{21}-/\sum C_{22}+$. Under the coaction of paleoclimate, organic matter input, and redox environment, the enrichment model of organic matter with high productivity and weak oxidation environment characteristics can also form excellent source rocks. This study is of great significance and provides theoretical guidance for the exploration of deep oil and gas resources.

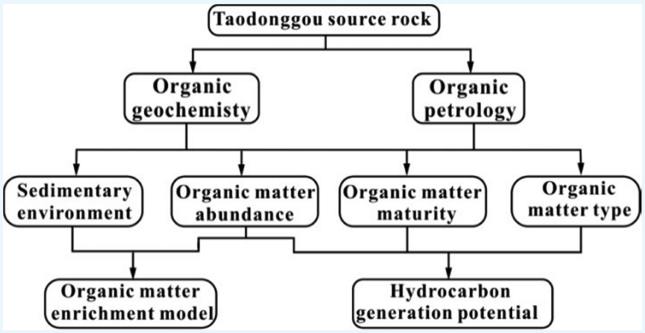

1. INTRODUCTION

Source rock is the material basis of the petroliferous basin. The quality of a source rock is often determined by the exploration and development of petroliferous basin. With the progress of exploration technology and the growing demand for energy,[1] it is difficult to meet the actual needs of social development with shallow oil and gas resources, so it is necessary to shift the focus of oil and gas exploration to deep, ultra deep, and unconventional oil and gas fields.[2−6]

The Middle Permian in Turpan-Hami basin has always been one of the important exploration strata in the Turpan-Hami oilfield. The discovered Lukeqin, Shanshan, and other oil- and gas-bearing structures show the good exploration potential of this set of strata.[7] The Middle Permian strata are widely distributed in Taibei sag, which has been rated as the key area for pre-Jurassic exploration in the Turpan-Hami oilfield by many resource evaluations.

Although the mudstone of the Middle Permian Taodonggou group in Taibei sag has been proved to be an effective source rock,[8] due to its deep burial, less drilling exposure, and poor quality of seismic data,[9] the exploration degree is low. In addition, the previous understanding of the organic geochemical characteristics and hydrocarbon generation potential

Received: July 30, 2021
Accepted: November 4, 2021
Published: November 16, 2021

https://doi.org/10.1021/acsomega.1c04061
ACS Omega 2021, 6, 31578−31594

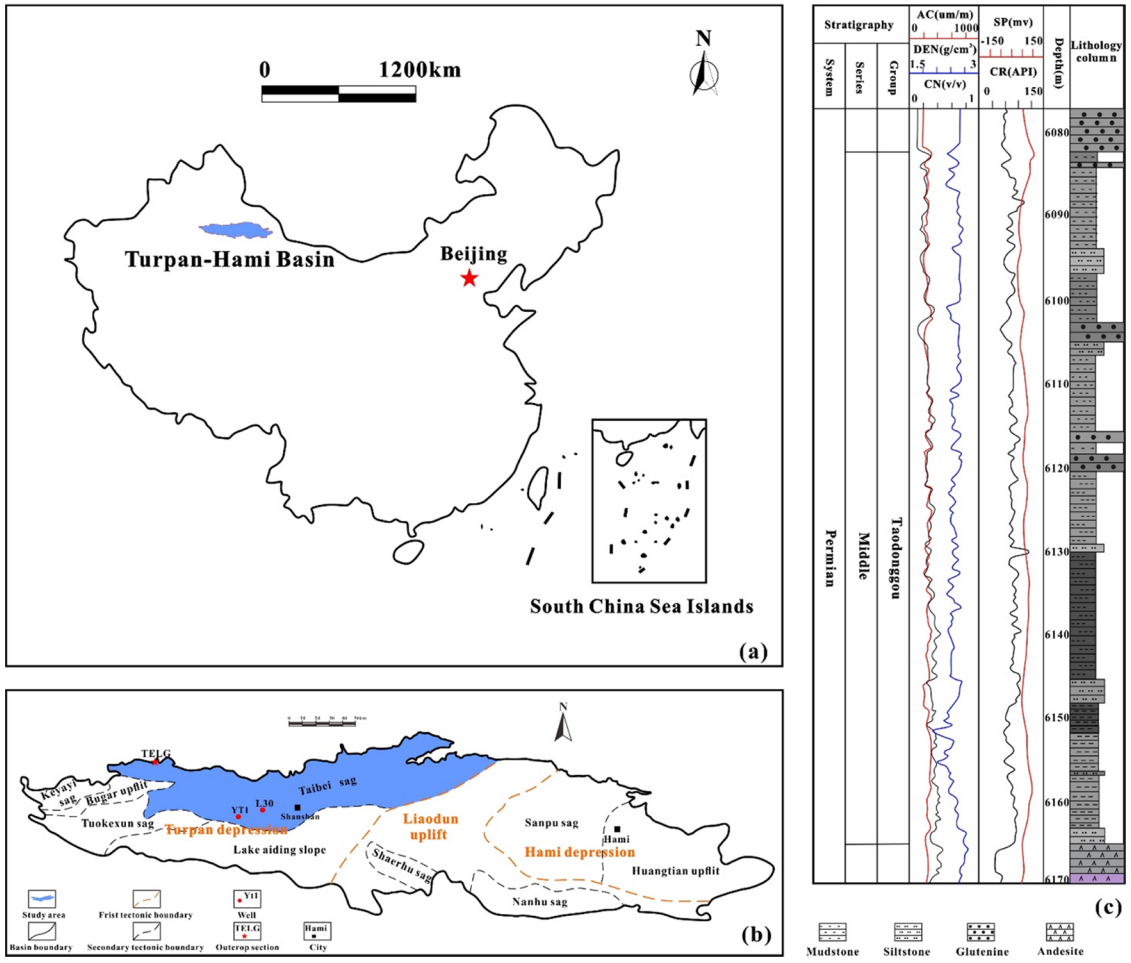

Figure 1. Geological overview of the Turpan-Hami Basin and of the study area: (a) location of the Turpan-Hami Basin; (b) tectonic units of the Turpan-Hami Basin and location of the study area;[7] and (c) stratigraphic column of the Permian Taodonggou group in YT1.

of this set of strata came from outcrops, which led to the lack of understanding of its geochemical characteristics.

Based on the latest drilling core and cuttings samples, this paper systematically revealed the organic petrology, geochemical characteristics, sedimentary environment, and hydrocarbon generation potential of Middle Permian Taodonggou source rocks in Taibei sag, Turpan-Hami basin, using organic petrology and organic geochemistry experiments, and analyzed the influence of the sedimentary environment on the enrichment of organic matter in source rocks.

2. GEOLOGICAL SETTING

Turpan-Hami basin is one of the important petroliferous basins in Northwest China (Figure 1a). It is a sedimentary basin developed on the folded basement of the Early Paleozoic. It has experienced the filling stage of fault depression in Permian Triassic and the evolution stage of the foreland basin since Jurassic.[10−12] From east to west, it can be divided into Hami depression, liaodun uplift, and Turpan depression[7] (Figure 1b).

Taibei sag is a secondary sag of Turpan Sag (Figure 1b), with an area of 9600 m^2. The latest seismic and drilling data show that there are carboniferous quaternary strata in the study area, with a maximum thickness of 9000 m. Among them, the Middle Permian Taodonggou group argillaceous source rocks are stably distributed in the study area (Figure 1c), with an average thickness of about 100 m and a burial depth ranging from 4000 to 6500 m.

3. SAMPLES AND EXPERIMENTS

Thirty-two mudstone samples of Taodonggou group were collected from the TELG profile, YT1 well, and L30 well, including 28 drilling samples (17 samples from the YT1 well and 11 samples from the L30 well) and 4 samples from the TELG profile. The whole-rock microcomponent, kerogen, vitrinite reflectance, rock-eval, Soxhlet extraction, and gas chromatography-mass spectrometry (GC-MC) were carried out.

According to the Chinese National Standard GB/T 16773-2008, the whole-rock macerals were measured and quantified by polarizing the microscopic system and hot stage (model: Axioskop 40, No.: 0700380Y). Based on the Chinese Industry Standard SYT 5124-2012, the vitrinite reflectance of Taodonggou group mudstone was obtained by an MSP UV−vis 2000 spectrometer. Based on the Chinese National Standard GB/T 18602-2012, the geochemical parameters of mudstone samples were obtained by a YQ-VII pyrometer. According to the Chinese National Standard GB/T 19145-2003, the total organic carbon content (TOC) of mudstone samples was determined by an ACS744 carbon sulfur analyzer. Chloroform asphalt "A" is determined by Soxhlet extraction. According to the China Petroleum Industry Standard SYT

https://doi.org/10.1021/acsomega.1c04061
ACS Omega 2021, 6, 31578−31594

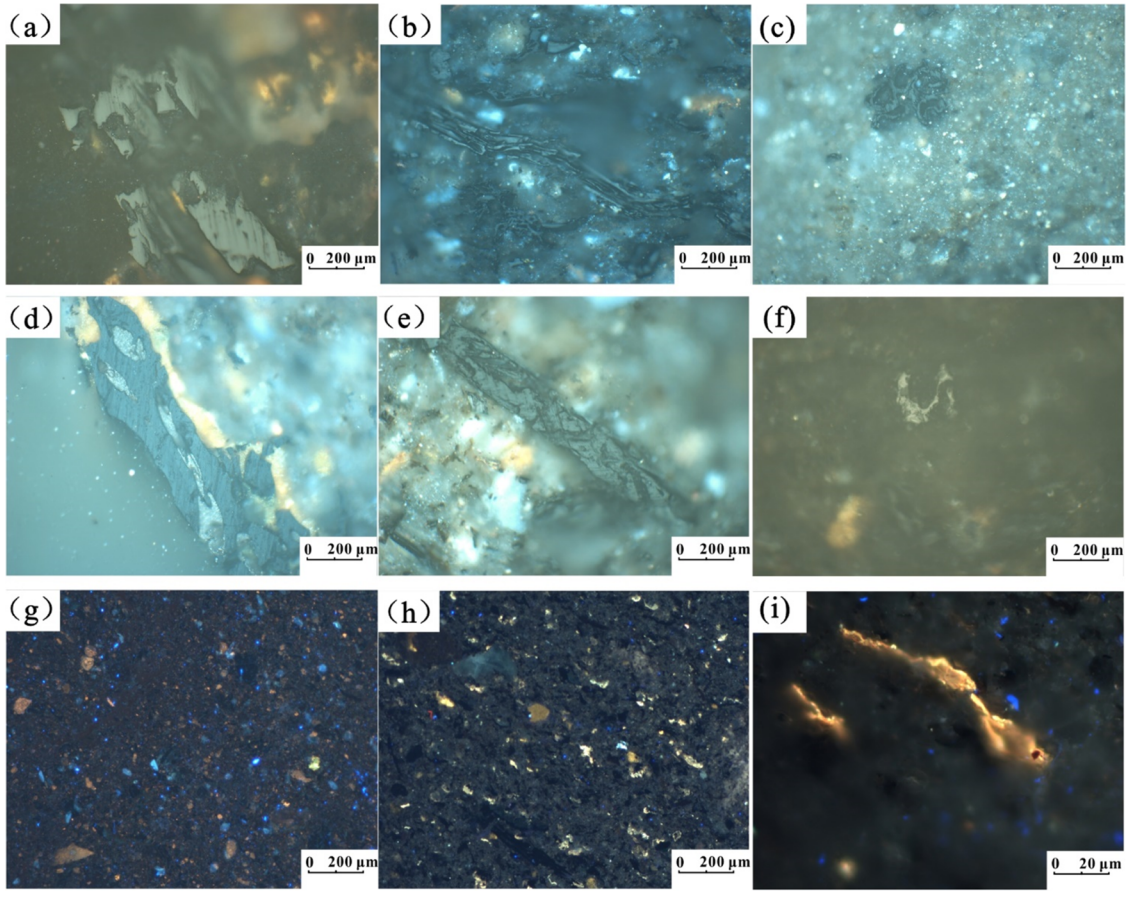

Figure 2. Maceral photos of source rocks of the Middle Permian Taodonggou group in Taibei sag: (a) Vitrodetrinite; (b) telinite 2; (c) telinite 2; (d) vitrodetrinite; (e) vitrodetrinite; (f) inerodetrinites; (g) exinite; (h) exinite; and (i) lamalginiite.

Table 1. Whole-Rock Macerals and Kerogen Macerals of Taodonggou Group Source Rocks in Taibei Sag

		whole-rock macerals			macerals of kerogen		
well and profile	depth (m)	vitrinite (%)	inertinite (%)	exinite (%)	vitrinite (%)	inertinite (%)	exinite + sapropelic (%)
L-30	5062.35				2	10	88
L-30	5013	74	2	24			
L-30	5030	62	15	23	11	46	43
L-30	5038	88	7	5			
L-30	5041	80	12	8			
L-30	5060	72	18	20	6	52	42
L-30	5064	60	25	15	7	41	52
L-30	5070	85	5	10	14	41	45
L-30	5076	90	4	6			
YT-1	6092	40	37	23			
YT-1	6140				8	23	69
YT-1	6142−6144	85	5	10	6	26	68
YT-1	6147	80	10	10	5	30	65
YT-1	6151	78	7	15	85	5	10
YT-1	6154				80	10	10
YT-1	6160−6162				78	7	15
YT-1	6144.7				15	23	62
YT-1	6145.3				58	4	38
YT-1	6145.8				12	53	35
TELG					42	20	38
TELG					33	28	39
TELG					40	18	42
TELG					30	12	58

https://doi.org/10.1021/acsomega.1c04061
ACS Omega 2021, 6, 31578−31594

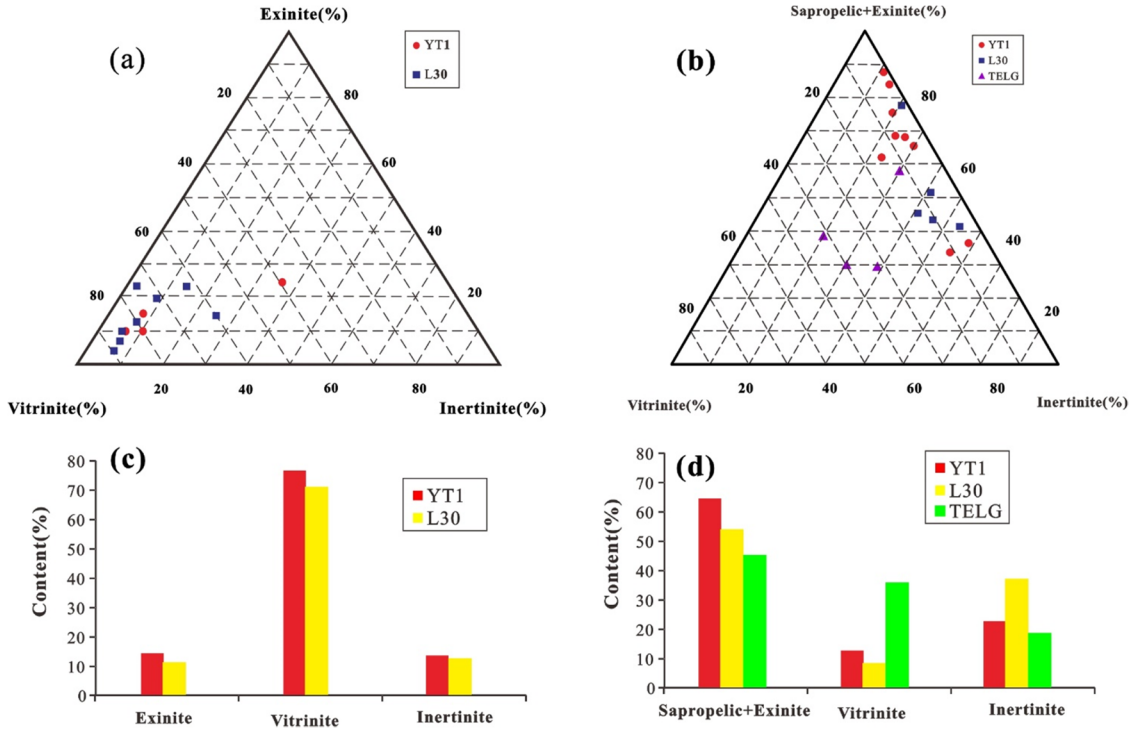

Figure 3. Whole-rock macerals and kerogen macerals: (a) trigonometry of whole-rock macerals; (b) trigonometry of kerogen macerals; (c) histogram of the whole-rock maceral content; and (d) histogram of the kerogen maceral content.

5118-2005, mudstone samples are crushed to less than 120 mesh and extracted for 72 h. The gas chromatography-mass spectrometry (GC-MC) experiment is completed by the Key Laboratory of Natural Gas Accumulation and Development of CNPC. The system consists of a high-temperature pyrolyzer produced by SGE company in Australia, a HP 5890A gas chromatograph produced by HP Company in the United States, and a microcomputer data system.

4. RESULTS

4.1. Organic Petrology. The vitrinite of source rocks in Taibei sag is turned from gray-white to gray-black under the reflected light of oil immersion, mainly composed of vitrodetrinite, and some of them contain telocollinite and telinite 2. The exinite is beige and orange-yellow in blue fluorescence, and it is mainly lamalginiite. The inertinite is grayish-white and mainly composed of inerodetrinites (Figure 2).

Table 1 shows the contents of whole-rock macerals and kerogen components of Taodonggou group source rocks.

The results of whole-rock maceral quantitative experiments show that the organic matter of Taodonggou group source rocks is mainly vitrinite, and the vitrinite content can reach 40−90%, with an average of 74.5%. The content of exinite ranges from 5 to 24%, with an average of 13.25%. The content of inertinite ranges from 2 to 37% (average = 12.25%). The content of vitrinite in the L-30 well is 60−90%, with an average of 76.4%. The content of exinite ranges from 5 to 24%, with an average of 12.6%. The content of inertinite ranges from 2 to 25% (average = 11%). The content of exinite in the YT-1 well ranges from 40 to 85%, with an average of 70.75%. The content of exinite ranges from 10 to 23%, with an average of 14.5%. The content of inertinite ranges from 5 to 37% (average = 11%) (Figure 3a,c).

A whole-rock analysis can only analyze morphological organic matter but cannot study and quantitatively analyze "amorphous" components,[13] so the whole-rock analysis cannot accurately quantify organic macerals of source rocks. If we want to find out the organic petrological characteristics of the source rocks of the Middle Permian Taodonggou group, we must purify the organic matter in the source rocks.

After purification of organic matter from mudstone samples, it is found (Figure 3b,d) that the main macerals of source rocks in Taodonggou group are exinite and sapropelite, with the content of 35−88% and an average value of 57.28%, followed by inertinite formations, with the content of 4−53% and an average value of 27.17%. The content of vitrinite ranges from 1 to 58%, with an average of 15.55%. In the L-30 well, the contents of exinite and sapropelite range from 42 to 88%, with an average value of 54%; the contents of inertinite range from 10 to 52%, with an average value of 38%; and the contents of vitrinite range from 2 to 14% (average = 8%). In the YT-1 well, the contents of exinite and sapropelite range from 35 to 88%, with an average value of 64.89%; the contents of inertinite range from 4 to 53% (average = 22.23%); and the contents of vitrinite range from 1 to 53%, with an average value of 12.79%. The contents of exinite and sapropelite in the TELG profile range from 38 to 58%, with an average value of 44.25%, the contents of inertinite range from 12 to 28% (average = 19.5%), and the contents of vitrinite range from 30 to 42%, with an average value of 36.25%.

Therefore, the organic matter of the Middle Permian source rocks in Taibei sag of Turpan-Hami basin is mainly sapropelite and exinite, the vitrinite is mainly vitrodetrinite, and the exinite is mainly lamalginiite.

4.2. Organic Geochemistry. Table 2 shows the geochemical characteristics of Taodonggou group source rocks, including total organic carbon (TOC), hydrocarbon gen-

https://doi.org/10.1021/acsomega.1c04061
ACS Omega 2021, 6, 31578−31594

Table 2. Geochemical Characteristics of Source Rocks of Taodonggou Group, Taipei Sag

well and profile	depth (m)	TOC (%)	S_1 (mg HC/g)	S_2 (mg HC/g)	PG (mg HC/g)	chloroform asphalt A (%)	T_{max} (°C)	R_o (%)
L-30	5062.35	4.32	0.2008	4.1837	4.3918	0.0949	447	1.18
L-30	5012−5014	2.01	7.1678	7.1432	14.3842	0.3351	329	1.124
L-30	5019	0.8	0.6679	1.519	2.2098	0.1899	343	1.141
L-30	5030	4.17	0.307	3.1118	3.436	0.3442	445	0.99
L-30	5038	3.44	0.2838	1.9624	2.3143		446	0.978
L-30	5048−5054	3.63	0.3631	2.1673	2.5474		444	0.926
L-30	5060	4.39	0.2563	2.2899	2.564	0.1875	443	0.824
L-30	5064	4.51	0.3595	3.5677	3.9384	0.2103	445	1.173
L-30	5070	3.45	0.3584	2.6268	2.9963		443	1.025
L-30	5074−5078	3.53	0.2253	2.6557	2.8871	0.059	444	1.134
L-30	5080	3.33	0.2191	2.4389	2.664	0.1282	444	1.004
YT-1	6077	0.66	0.2547	0.5702	0.8429	0.0791	432	0.937
YT-1	6084	0.55	0.2399	1.0558	1.3		432	0.922
YT-1	6092	0.73	0.2512	1.0861	1.3411		429	1.137
YT-1	6102	0.86	0.2351	1.1887	1.4285		403	1.201
YT-1	6110−6116	0.66	0.2224	1.1053	1.3312	0.0791	448	1.29
YT-1	6122	0.71	0.3232	1.6788	2.0088		422	0.94
YT-1	6126−6132	1.07	0.4221	2.2339	2.6581	0.1377	444	1
YT-1	6136	0.95	0.4221	2.3554	2.7796		440	1.15
YT-1	6140	5.37	0.7973	3.9698	4.7785		465	1.32
YT-1	6142−6144	4.03	0.7681	3.5093	4.2846	0.3428	452	1.34
YT-1	6147	4.2	1.2098	5.0547	6.2746		450	1.201
YT-1	6151	0.92	0.3466	2.12	2.4722	0.1608	438	0.94
YT-1	6154	0.83	0.2831	1.6397	1.929	0.1303	393	1.07
YT-1	6160−6162	0.58	0.3739	1.6608	2.0364	0.1042	389	1.05
YT-1	6144.7	1.21	0.1342	0.643	0.7783	0.8767	468	1.26
YT-1	6145.3	3.18	1.6712	6.192	7.8632	0.7095	464	1.49
YT-1	6145.8	2.94	0.4151	2.0075	2.4351		464	1.04
TELG		0.66	0.1903	2.0005	2.1948	0.046	446	0.53
TELG		3.29	1.125	13.9591	15.0897	0.1463	445	0.65
TELG		2.43	0.4942	13.4866	13.9873	0.1904	448	0.55
TELG		5.13	0.7543	30.0974	30.8658	0.2439	455	0.62

eration potential (PG), chloroform asphalt A, maximum pyrolysis peak temperature (T_{max}), hydrogen index (HI), and vitrinite reflectance (R_o).

Rock-evals and Soxhlet extraction experiments show that the TOC value of the Middle Permian Taodonggou group source rocks in Taibei sag ranges from 0.55 to 6.08%, with an average value of 2.58 wt %. The hydrocarbon generation potential (PG) ranges from 0.78 mg HC/g to 30.86 mg HC/g, with an average value of 4.88 mg HC/g. Chloroform asphalt A ranges from 0.046 to 0.8767% (average = 0.2358%). The TOC value of the L30 well ranges from 0.8 to 4.51 wt %, with an average value of 3.416 wt %; the distribution of hydrocarbon generation potential ranges from 2.201 to 14.382 mg HC/g, with an average value of 4.286 mg/g; and chloroform asphalt A ranges from 0.059 to 0.3442 wt % (average = 0.1936%) (Figure 4a−c). The TOC value of the YT1 well ranges from 0.53 to 6.081 wt %, with an average value of 1.902 wt %; the distribution of hydrocarbon generation potential ranges from 0.77 to 8.306 mg HC/g, with an average value of 2.76 mg HC/g; and chloroform asphalt A ranges from 0. 0791 to 0.8767 wt % (average = 0.3176 wt %) (Figure 4d−f). The TOC value of the TELG profile ranges from 0.66 to 5.13 wt %, with an average value of 2.88 wt %; the hydrocarbon generation potential distribution ranges from 2.19 to 30.86 mg HC/g, with an average value of 15.53 mg HC/g; and chloroform asphalt A ranges from 0.046 to 0.2439 wt % (average = 0.1567 wt %) (Figure 4g−i). According to the TOC value, the abundance of organic matter in the L30 well is higher than that in the TELG profile and YT1 well. According to the hydrocarbon generation potential (PG), organic matter abundance in the TELG profile is higher than that in L30 and YT1 wells. According to chloroform asphalt *A*, organic matter abundance in the YT1 well is higher than that in the TELG profile and L30 well. Compared with the organic matter abundance of TELG outcrop and drilling samples, the results show that weathering has little or no impact on TELG profile samples.

The maximum pyrolysis temperature (T_{max}) of source rocks in Taibei sag ranges from 329 to 468 °C (average = 434.375 °C); the maximum pyrolysis temperature (T_{max}) of the L-30 well ranges from 329 to 447 °C, with an average value of 422.6 °C; the maximum pyrolysis temperature (T_{max}) of the YT1 well ranges from 389 to 468 °C, with an average value of 437.235 °C; and the maximum pyrolysis temperature (T_{max}) of the TELG profile ranges from 445 to 455 °C, with an average value of 448.5 °C (Figure 5a−c).

The vitrinite reflectance (R_o) of source rocks in Taibei sag ranges from 0.53 to 1.49%, with an average value of 1.048%. Among them, the vitrinite reflectance (R_o) of the L-30 well ranges from 0.824 to 1.173%, with an average value of 1.04%. The vitrinite reflectance (R_o) of the YT1 well ranges from 0.94 to 1.49%, with an average value of 1.168%. The vitrinite reflectance (R_o) of the TELG profile ranges from 0.53 to 0.65%, with an average value of 0.588% (Figure 6a−c).

https://doi.org/10.1021/acsomega.1c04061
ACS Omega 2021, 6, 31578−31594

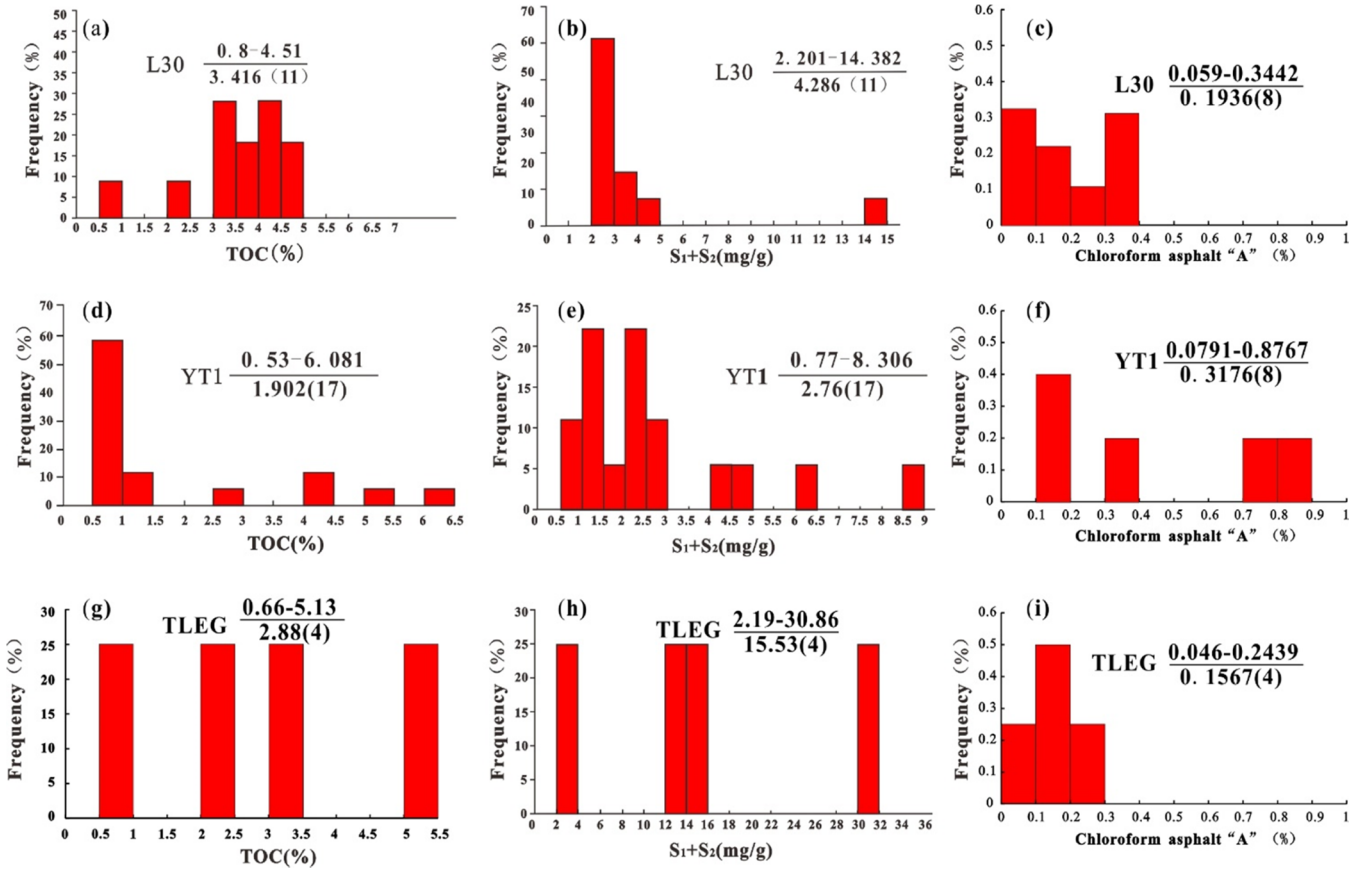

Figure 4. Frequency distribution histogram of organic matter abundance in source rocks of Taodonggou group in Taibei sag: (a–c) the frequency distribution histogram of TOC, PG, and chloroform asphalt A in the L-30 well, respectively; (d–f) the frequency distribution histogram of TOC, PG, and chloroform asphalt A in the YT-1 well respectively; and (g–i) the frequency distribution histogram of TOC, PG, and chloroform asphalt A in the TELG profile, respectively.

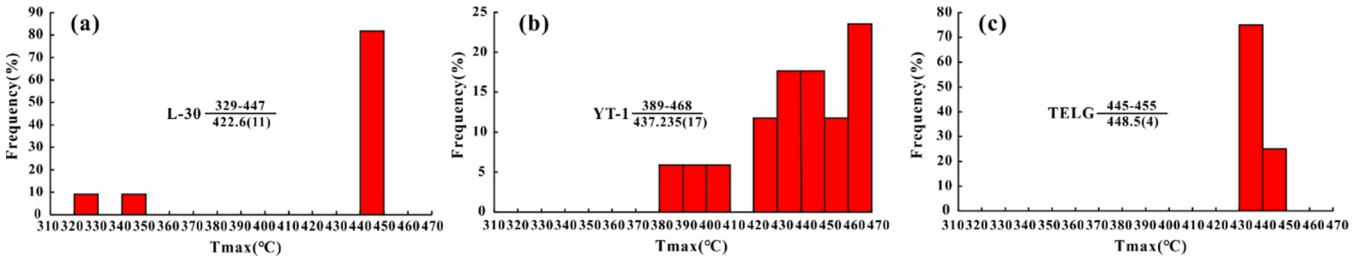

Figure 5. Frequency distribution histogram of T_{max} in source rocks of Taodonggou group in Taibei sag: (a) L-30 well, (b) YT-1 well, and (c) TELG profile.

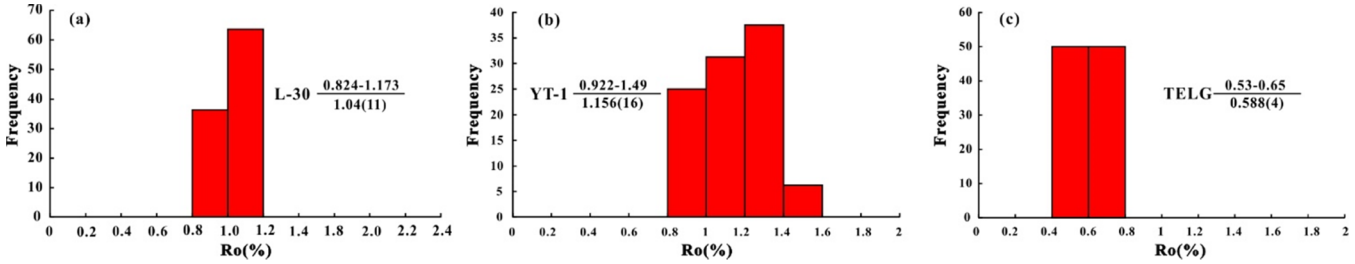

Figure 6. Frequency distribution histogram of R_o in source rocks of Taodonggou group in Taibei sag: (a) L-30 well, (b) YT-1 well, and (c) TELG profile.

4.3. Biomarker Compounds. Table 3 shows the biomarker characteristics of 15 mudstone samples from Taodonggou group in the study area, including *n*-alkanes, isoprene alkanes, steranes, and terpanes.

https://doi.org/10.1021/acsomega.1c04061
ACS Omega 2021, 6, 31578–31594

Table 3. Biomarkers of Source Rocks in Taodonggou Group, Taibei Sag

				n-alkanes				isoprene like alkanes		sterane								terpane	
well and profile	depth (m)	C no. range	main peak C no.	CPI	0EP	$\sum C_{21-}/\sum C_{22+}$	Pr/Ph	Pr/nC_{17}	Ph/nC_{18}	C_{27} (%)	C_{28} (%)	C_{29} (%)	C_{29} 20S/(20R + 20S)	C_{29} $\beta\beta/(\alpha\alpha + \beta\beta)$	C_{19}/C_{23}	C_{20}/C_{23}	C_{24}/C_{23}	T_s/T_m	C_{29}/C_{30}	GI
YT1	6110–6116	14–38	29	1.42	1.42	0.30	1.16	1.08	0.46	21.67	21.28	57.05	0.31	0.52	0.90	1.56	0.52	0.30	0.51	0.36
YT1	6126–6132	13–38	18	1.41	0.78	0.75	1.14	0.36	0.25	21.41	14.37	64.22	0.31	0.53	1.01	1.63	0.48	0.50	0.50	0.22
YT1	6142–6144	14–37	18	1.30	0.86	0.59	1.16	0.35	0.26	28.25	13.52	58.23	0.33	0.48	1.00	1.51	0.55	0.54	0.48	0.20
YT1	6144.70	15–37	18	1.14	0.98	1.01	0.81	0.17	0.17	41.20	22.31	36.49	0.49	0.48	0.15	0.44	0.60	0.47	0.63	0.22
YT1	6145.30	13–37	17	1.12	0.99	2.26	2.93	0.19	0.07	40.20	21.31	38.49	0.42	0.49	1.01	0.84	0.76	0.55	0.43	0.76
YT1	6145.80	13–37	17	1.05	0.99	1.88	1.70	0.17	0.10	44.43	18.15	37.42	0.35	0.53	0.45	0.59	0.69	0.58	0.77	0.32
YT1	6154.00	14–41	29	1.32	1.33	0.39	0.94	0.47	0.43	27.09	12.17	60.74	0.32	0.52	1.04	1.25	0.51	0.51	0.49	0.22
YT1	6160–6162	14–40	29	1.35	1.34	0.41	0.94	0.65	0.53	28.86	11.04	60.10	0.34	0.60	0.78	1.31	0.53	0.51	0.48	0.24
L30	5048–5054	14–35	19	1.21	1.02	0.78	1.44	0.79	0.48	27.11	15.66	57.23	0.37	0.58	0.41	0.55	0.55	0.55	0.74	0.23
L30	5062.35	14–33	18	1.32	0.96	0.82	1.97	0.72	0.31	29.24	15.32	55.44	0.28	0.64	0.60	1.72	0.45	0.76	0.74	0.16
L30	5074–5078	14–35	23	1.34	1.22	0.58	1.68	0.92	0.41	30.47	14.43	55.10	0.32	0.55	0.86	1.87	0.48	0.56	0.83	0.20
TELG		13–29	21	1.57	1.36	1.17	1.54	0.50	0.33	35.08	20.25	44.67	0.36	0.31	0.46	0.54	0.60	2.02	0.34	0.16
TELG		13–30	23	1.30	1.30	1.13	1.82	0.99	0.65	21.89	20.94	57.17	0.36	0.53	0.56	0.63	0.69	1.78	0.35	0.18
TELG		13–30	21	1.26	1.33	1.18	1.89	0.73	0.42	45.83	17.02	37.15	0.44	0.45	0.38	0.56	0.49	1.60	0.32	0.16
TELG		13–30	19	1.29	1.30	1.88	2.06	0.51	0.30	30.41	22.50	47.09	0.41	0.42	0.31	0.54	0.46	2.12	0.36	0.13

https://doi.org/10.1021/acsomega.1c04061
ACS Omega 2021, 6, 31578−31594

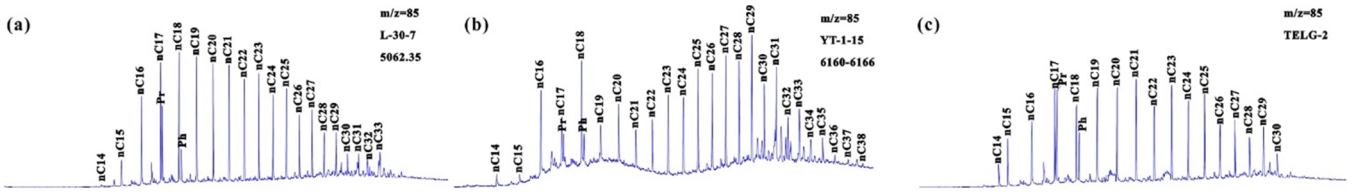

Figure 7. Mass spectrometric analysis of *n*-alkanes (m/z 85) in saturated hydrocarbon components of Taodonggou group source rocks: (a) L-30 well, (b) YT-1 well, and (c) TELG profile.

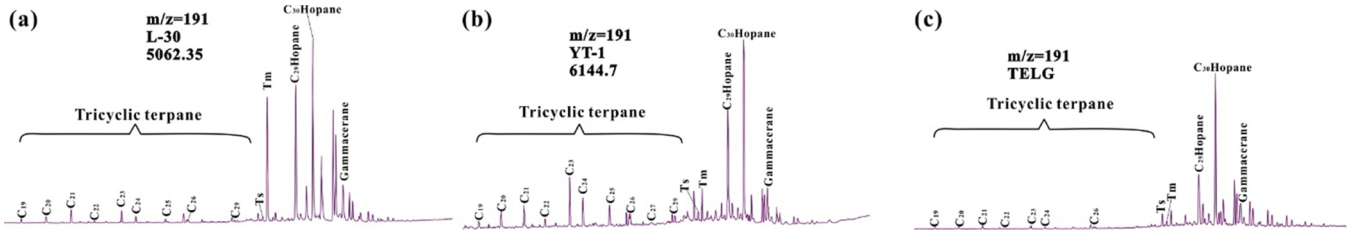

Figure 8. Mass spectrometric analysis of terpanes (m/z 191) in saturated hydrocarbon components of Taodonggou group source rocks: (a) L-30 well, (b) YT-1 well, and (c) TELG profile.

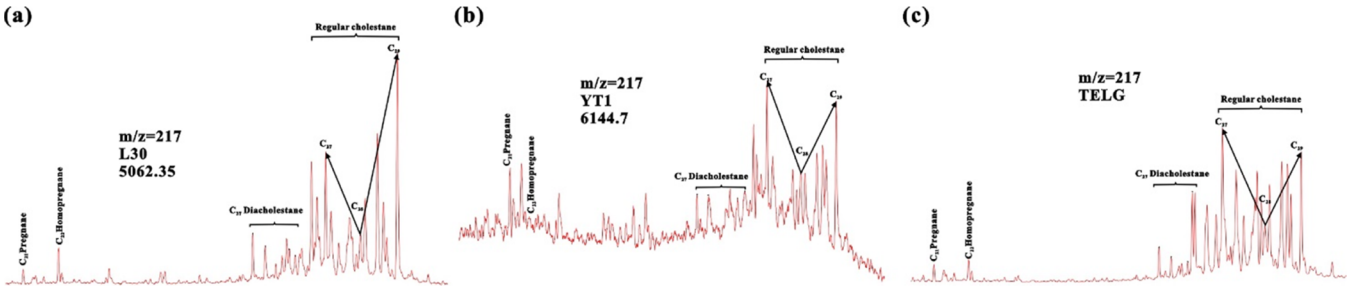

Figure 9. Mass spectrometric analysis of f sterane (m/z 217) in saturated hydrocarbon components of Taodonggou group source rocks: (a) L-30 well, (b) YT-1 well, and (c) TELG profile.

4.3.1. Straight Chain Alkanes. The carbon number of *n*-alkanes in Taodonggou group source rocks in Taibei sag ranges from nC_{13} to nC_{40}, with the main peaks of nC_{17}, nC_{18}, nC_{19}, nC_{21}, nC_{23}, and nC_{29}. The short chains and ratio ($\sum C_{21-}/\sum C_{22+}$) range from 0.3 to 2.26, with an average value of 1.009. The carbon preference index (CPI) ranged from 1.05 to 1.57, with an average value of 1.294. The odd−even predominance index (OEP) ranged from 0.78 to 1.42, with an average value of 1.145 (Figure 7).

4.3.2. Isoprenoids. Pristane (Pr) and phytane (Ph) can indicate the input and depositional environment of organic matter and are widely used parameters in isopren-like alkanes.[14,15] The distribution of Pr/Ph of Taodonggou group source rocks in the study area ranges from 0.94 to 2.93, with an average value of 1.546, that of Pr/nC_{17} ranges from 0.17 to 1.08, with an average value of 0.574, and that of Ph/nC_{18} ranges from 0.25 to 0.46, with an average value of 0.345.

4.3.3. Terpanes. On the m/z = 191 mass chromatogram (Figure 8), terpenoids were mainly composed of gammacerane, moretane, homohopanes (C_{31}−C_{35}), 17α(H)-trisnorhopane (Tm), 18α(H)-trisnorhopane (Ts), tricyclic terpanes, tetracyclic terpane, and pentacyclic terpanes. The relative content of homohopanes is a positive sequence, that is, C_{31} > C_{32} > C_{33} > C_{34} > C_{35} homohopane, especially, C_{34} homohopane and C_{35} homohopane are very low.

The abundance of C_{30} hopane is higher than that of C_{29} hopane in all samples, and the C_{29}/C_{30} hopane ratio ranges from 0.32−0.83 (Table 3), with an average value of 0.53. The ratio of C_{19}/C_{23} tricyclic terpane, C_{20}/C_{23} tricyclic terpane, and C_{24}/C_{23} tricyclic terpane ranges from 0.31 to 1.04 (average = 0.66), 0.44 to 1.87 (average = 1.04), and 0.46 to 0.76 (average = 1.04), respectively. The ratio of T_s/T_m ranges from 0.3 to 2.12 (average = 0.89) and that of YT1 and L30 wells show low values (0.3−0.76, with an average value of 0.53, less than 1), indicating that the organic matter of YT1 and L30 wells is in the mature stage; however, the ratio of the T_s/T_m value of the TELG profile ranges from 1.6 to 2.12 (average = 1.88), which indicates that the organic matter of the TELG profile is in the immature−mature stage[16] (Table 3).

Gammacerane is present in all Taodonggou samples (Figure 8 and Table 3), and the gammacerane index (GI) ranges between 0.13 and 0.76, with an average value of 0.25. This suggests syn-depositional water column salinity stratification.[17]

4.3.4. Steroids. All samples of Taodonggou group in Taibei sag share similar sterane distribution patterns. Cholestane series compounds outsize pregnane series compounds. The distributions of regular steranes C_{27}−C_{28}−C_{29} show asymmetrical V-shaped and reverse L-shaped features in all samples (Figure 9). The relative proportion of $\alpha\alpha\alpha C_{29}$sterane (*R*) is the highest (37.15−64.22% with an average value of 51.11%), followed by C_{27} (21.41−45.83% with an average value of 31.54%) and C_{28} steranes (13.52−22.5% with an average value of 17.35%).

The ratio of $C_{29}\alpha\alpha\alpha$20S/(20S + 20R) sterane isomerization ranges from 0.28 to 0.49, while that of $C_{29}\beta\beta/(\beta\beta + \alpha\alpha)$

https://doi.org/10.1021/acsomega.1c04061
ACS Omega 2021, 6, 31578−31594

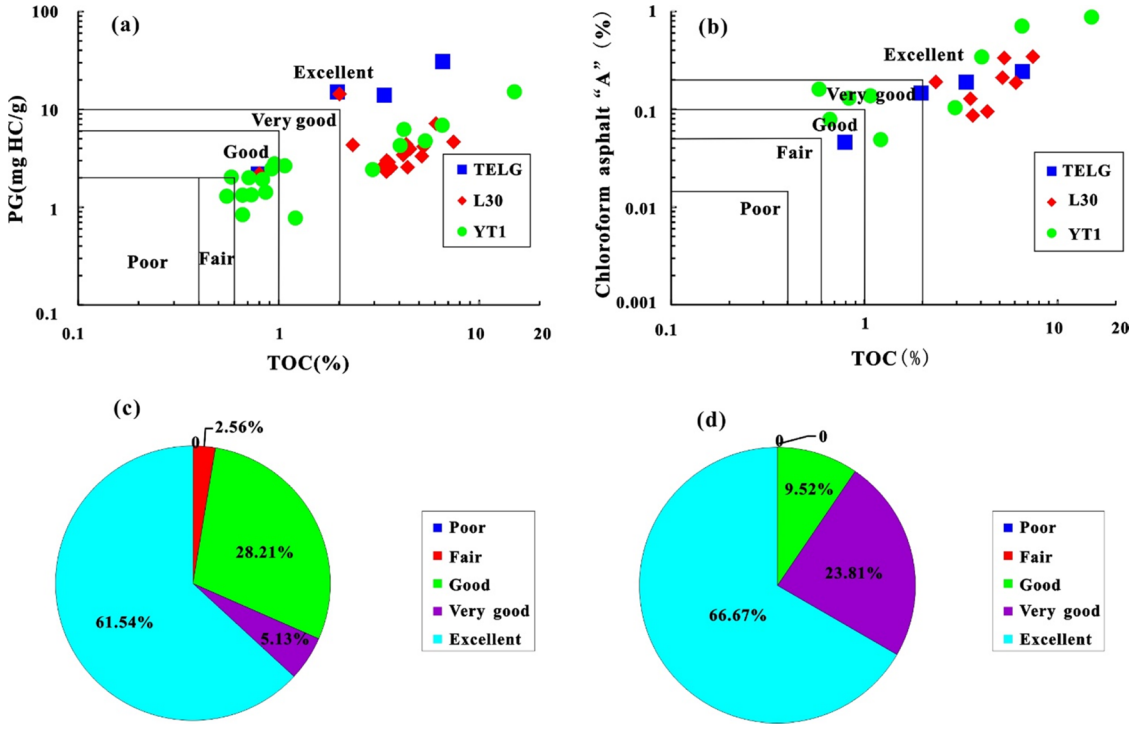

Figure 10. Evaluation of source rocks in Taodonggou group of Middle Permian: (a) cross plot of TOC and PG (modified after 22); (b) cross plot of TOC and chloroform asphalt A (modified after 20); (c) according to the cross plot of TOC and PG, the fan chart of hydrocarbon source rock grade is shown; and (d) according to the cross plot of TOC and chloroform asphalt A, the fan chart of hydrocarbon source rock grade is shown.

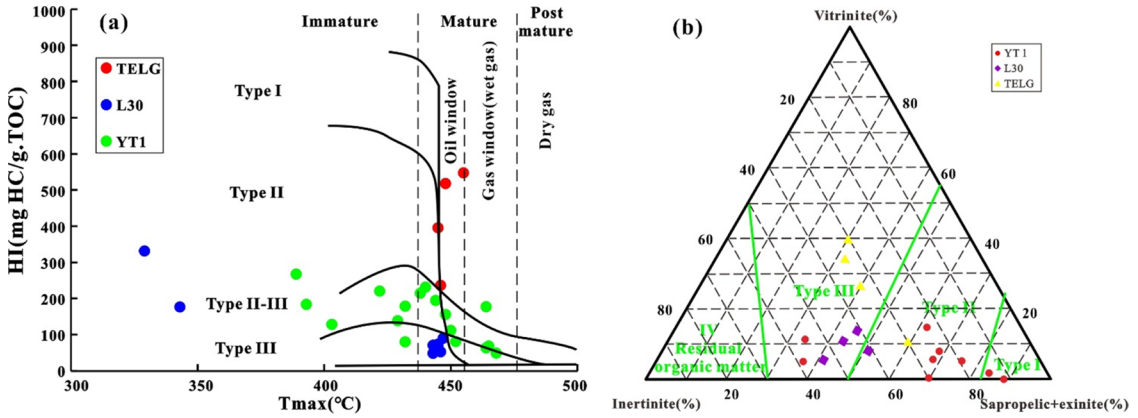

Figure 11. Types of organic matter in source rocks of Taodonggou group in Taibei sag: (a) cross plot of HI and T_{max} (modified after 24) and (b) microcomponent triangulation (modified after 27).

sterane isomerization varies from 0.31 to 0.64 (Table 3), which indicate a high thermal maturity.[18]

5. DISCUSSION

The characteristics of organic petrology and organic geochemistry are of great importance to the evaluation of hydrocarbon generation potential of source rocks.[19] Therefore, it is necessary to analyze and further reveal the abundance, type, maturity, parent material sedimentary environment of source rocks, and the influence of the parent material sedimentary environment on the occurrence of organic matter.

5.1. Organic Matter Evaluation. *5.1.1. Abundance.* Organic matter abundance is the material basis of hydrocarbon formation in source rocks, and it is also the most basic parameter to evaluate the quality of source rocks.[20] The parameters commonly used to evaluate the organic matter abundance of source rocks are total organic carbon content (TOC), total hydrocarbon content (HC), hydrocarbon generation potential (PG), and chloroform asphalt A.[21−23]

According to the total organic carbon (TOC) and hydrocarbon generation potential (PG), Taodonggou group source rocks are mainly distributed in poor to excellent source rocks, in which poor source rocks account for 2.56%, good source rocks account for 28.21%, very good source rocks account for 5.15%, and excellent source rocks account for 61.54% (Figure 10a,c). According to the total organic carbon (TOC) and chloroform asphalt A, the source rocks of Taodonggou group in the study area are mainly distributed in good to excellent source rocks, with good source rocks accounting for 9.52%, very good source rocks accounting for 23.82%, and excellent source rocks accounting for 66.67% (Figure 10b,d). In conclusion, the source rocks of Taodonggou

https://doi.org/10.1021/acsomega.1c04061
ACS Omega 2021, 6, 31578−31594

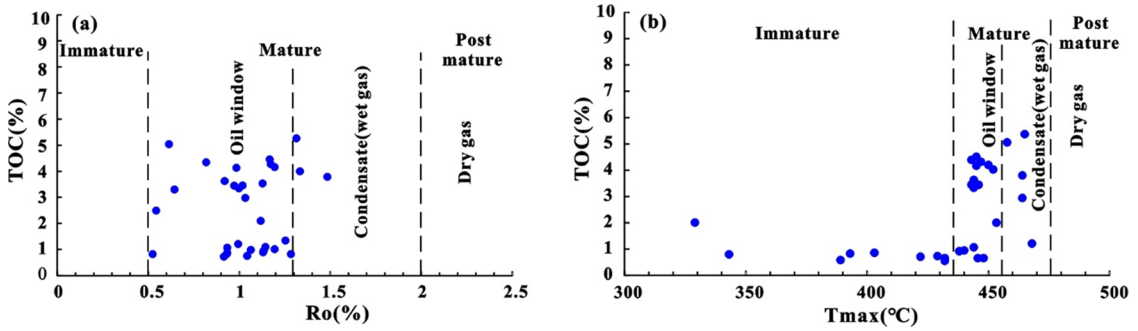

Figure 12. Maturity of organic matter in source rocks of Taodonggou group in Taibei sag: (a) cross plot of TOC and R_o and (b) cross plot of TOC and T_{max}.

group in the study area are mainly excellent source rocks. This indicates that the source rocks of Taodonggou group in Taibei Sag have a good hydrocarbon generation potential.

5.1.2. Type. The difference of organic matter types will affect the hydrocarbon generation potential and products of source rocks.[21,24] There are many evaluation indexes of organic matter types, such as kerogen element composition, kerogen maceral composition and its type index, relative composition of steranes, and rock pyrolysis hydrogen index (HI)−oxygen index (OI).[24−28]

The cross plot of T_{max} and HI (Figure 11a) shows that the organic matter types of Taodonggou group source rocks are mainly type III and types II−III, and some of them are type II and type I. In addition, kerogen macerals also show that the organic matter types of Taodonggou group source rocks are mainly type III and type II (Figure 11b), which are consistent with the results of T_{max} and HI cross plot. It can be concluded that the organic matter types of Taodonggou group source rocks are mainly type III and types II−III. This indicates that the source rocks of Taodonggou group in Taibei sag have good gas and oil generation capacity.

5.1.3. Maturity. The maturity of organic matter is the key to generate a large amount of oil or natural gas. R_o and T_{max} are important indicators of organic matter maturity.[28−31] Previous studies have found that for continental mudstone, vitrinite reflectance (R_o) is the best index, followed by T_{max}.[29] However, T_{max} can be used as a very good maturity index when organic matter types are III and II.[29−31] Generally speaking, R_o < 0.5% or T_{max} < 435 °C is the immature stage; 0.5% < R_o < 1.3% or 435 °C < T_{max} < 455 °C is the oil window stage; 1.3% < R_o < 2% or 455 °C < T_{max} < 475 °C is the condensate (wet gas) stage; and R_o > 2.0% or T_{max} > 475 °C is the postmature (dry gas) stage.[24,25,29]

In an advanced analysis based on the intersection diagrams of Ro and TOC (Figure 12a), T_{max} and TOC (Figure 12b) of Taodonggou group source rocks in the study area are drawn, respectively. The results suggest that the Middle Permian source rocks in Taibei sag are in the mature stage, most of them are distributed in the oil window stage, and a small amount are distributed in the condensate (wet gas) stage. This shows that the source rocks of Taodonggou group are mainly oil generating at present.

5.2. Sedimentary Environment. *5.2.1. Paleoclimate.* Paleoclimate has an important influence on source rocks.[32] Previous studies have found that the carbon preference index (CPI) of source rocks can indicate the degree of dryness and wetness of paleoclimate. Taking CPI = 1 as the boundary, the smaller the CPI value, the higher the degree of wetness.[33−35] The CPI value of source rocks ranges from 1.05 to 1.57, with an average value of 1.294, which is similar to the CPI value of source rocks of Meishan formation in Yinggehai basin,[34] and it is in a semihumid and semiarid climate, which is basically consistent with the previous results based on the annual ring of lignified stone.[36] Therefore, Taodonggou source rock was formed in semihumid and semiarid environment.

5.2.2. Organic Matter Input. The main peak carbon of *n*-alkanes can indicate the input of organic matter.[37−40] When the main peak carbon is low carbon number (<20), it indicates the source of algae and other lower aquatic organisms. When the carbon number is high (>C_{23}), the distribution characteristics of the peak type indicate the input of terrestrial higher plants.[38,39] The main carbon peaks of Taodonggou group source rocks in the study area are nC_{17}, nC_{18}, nC_{19}, nC_{21}, nC_{23}, and nC_{29}, indicating that the organic matter input of the source rocks is mixed source input, and the ratio $\sum C_{21}-/\sum C_{22}+$ of source rocks can characterize the relative input of lower aquatic organisms and terrestrial higher plants.[39] The ratio $\sum C_{21}-/\sum C_{22}+$ of the source rocks ranges from 0.3 to 2.26 in the study area, with an average value of 1.009. It shows that the input amount of aquatic organisms is equal to that of terrestrial higher plants. According to the relationship between the ratio $\sum C_{21}-/\sum C_{22}+$ and depth (Figure 13), it is found that the terrigenous higher plant input is dominant in the early stage of Taodonggou group, the lower aquatic organism input is dominant in the middle stage, and the terrigenous higher plant input is dominant in the late stage.

The relative composition of C_{27}, C_{28}, and C_{29} regular steranes can reflect the source of organic matter input. Previous studies have found that C_{27} sterane indicates the source of aquatic organisms, C_{28} sterane is related to diatoms, and C_{29} sterane indicates the source of higher organisms.[40−44] According to the regular sterane triangle of $C_{27}-C_{28}-C_{29}$ (Figure 14), the source rocks of Taodonggou group are mainly distributed in estuarine bay and terrestrial, and a few are distributed in open marines. The corresponding biological sources are plankton and terrestrial higher plants.[44] The results also show that the organic matter input of source rocks of Taodonggou group has the characteristics of a mixed source.

In addition, tricyclic terpanes and tetracyclic terpanes are also important biomarkers of terrestrial organic matter input.[42,43] It is generally believed that the higher the ratio of C_{19}/C_{23} tricyclic terpane and C_{20}/C_{23} tricyclic terpane, the higher the terrestrial organic matter input. The ratio of C_{19}/C_{23} tricyclic terpane did not change significantly in the study area (vary from 0.15 to 1.04, with an average value of 0.66), which cannot prove that the source of organic matter is the mixed

https://doi.org/10.1021/acsomega.1c04061
ACS Omega 2021, 6, 31578−31594

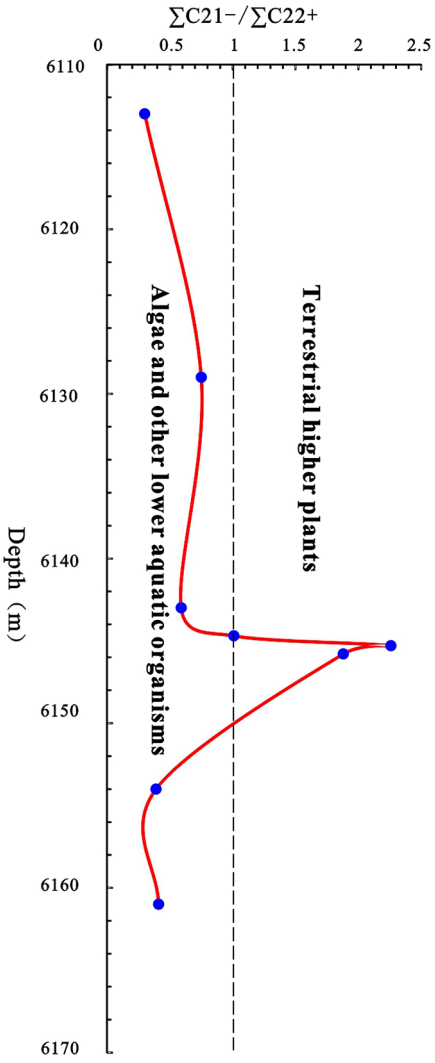

Figure 13. Organic matter input from source rocks of Taodonggou group in Taibei sag.

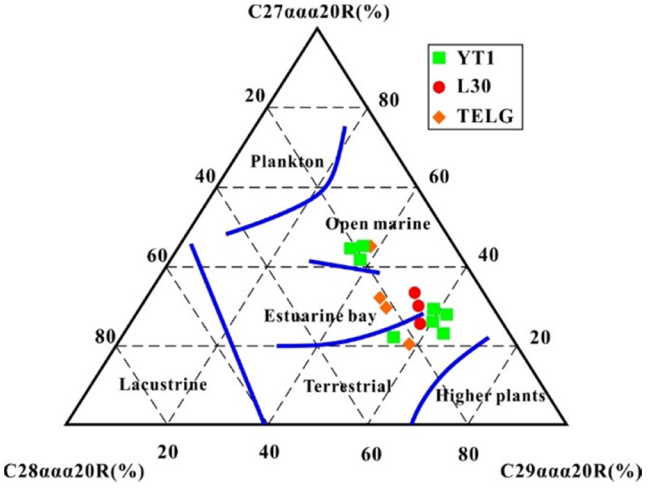

Figure 14. Triangles of *n*-steranes (C_{27}−C_{28}−C_{29}) in source rocks of Taodonggou group, Middle Permian (modified after 44).

source. However, the ratio of C_{20}/C_{23} tricyclic terpane changed obviously and has the characteristics of segmentation, which is basically consistent with the result expressed by the main peak carbon of *n*-alkanes.

In conclusion, the organic matter of source rocks of Taodonggou group is input as a mixed source. The early and late stage is dominated by terrestrial higher plants. The middle stage is dominated by lower aquatic organisms.

5.2.3. Redox Environment. Oxidation−reduction condition is one of the important factors affecting the preservation of organic matter, and the strength of reducibility determines the degree of destruction of organic matter by biochemical action.[41,42] Previous studies have found that the ratio of pristane (Pr) to phytane (Ph) can indicate the oxidation−reduction environment: Pr/Ph < 0.8 indicates a strong reduction environment, 0.8 ≤ Pr/Ph < 3 indicates weak reduction and weak oxidation environments, and Pr/Ph ≥ 3 indicates the oxidation environment.[41−44] The Pr/Ph source rocks of Taodonggou group in the study area mainly range from 0.94 to 2.93, with an average value of 1.546, which indicates that the source rocks in the study area are deposited in a weak reduction and weak oxidation environment.

In addition, Pr/nC_{17} and Ph/nC_{18} can be used to restore the properties of paleowater and indicate the type of kerogen.[45] The intersection diagram of Pr/nC_{17} and Ph/nC_{18} (Figure 15) shows that the source rocks of Taodonggou group are deposited in a weak redox environment, which is a transitional environment. The results are basically consistent with Pr/Ph.

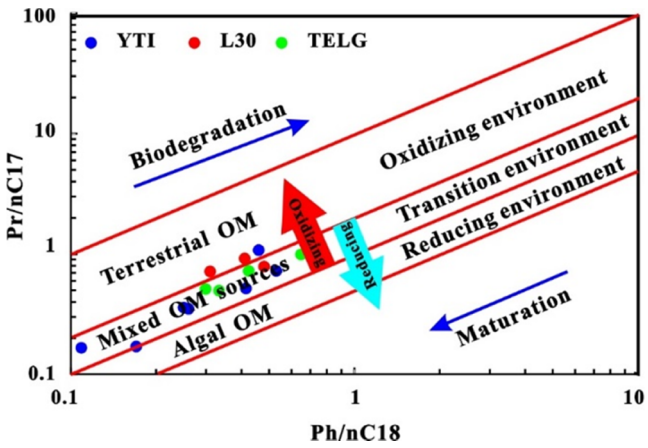

Figure 15. Cross plot of Pr/nC_{17} and Ph/nC_{18} of Taodonggou group, Middle Permian (modified after 45).

5.3. Influence of Sedimentary Environment on Organic Matter Enrichment. The enrichment degree of organic matter depends on the content of original organic matter and preservation conditions.[45−51] The content of original organic matter is mainly affected by the flourishing degree of Paleontology and the filling of terrigenous detritus, and these factors are closely related to the sedimentary environment. To explore the influence of the sedimentary environment on the enrichment of organic matter in Taibei sag, this study analyzed the paleoclimate, organic matter input, and oxidation−reduction conditions.

5.3.1. Influence of Paleoclimate on Organic Matter Enrichment. To explore the influence of paleoclimate on the abundance of organic matter, the relationship between CPI and TOC and PG and chloroform asphalt A is drawn (Figure 16). The results show that CPI has a weak negative correlation with TOC, PG, and chloroform asphalt A in the study area,

https://doi.org/10.1021/acsomega.1c04061
ACS Omega 2021, 6, 31578−31594

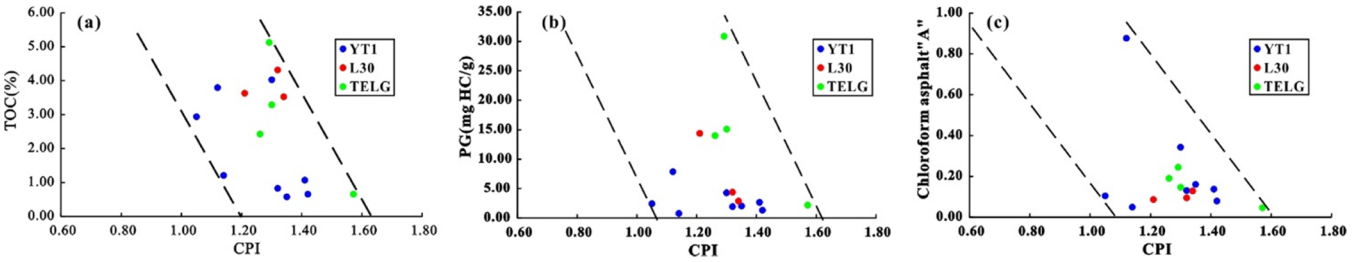

Figure 16. Relationship between CPI and (a) TOC, (b) PG, and (c) chloroform asphalt A.

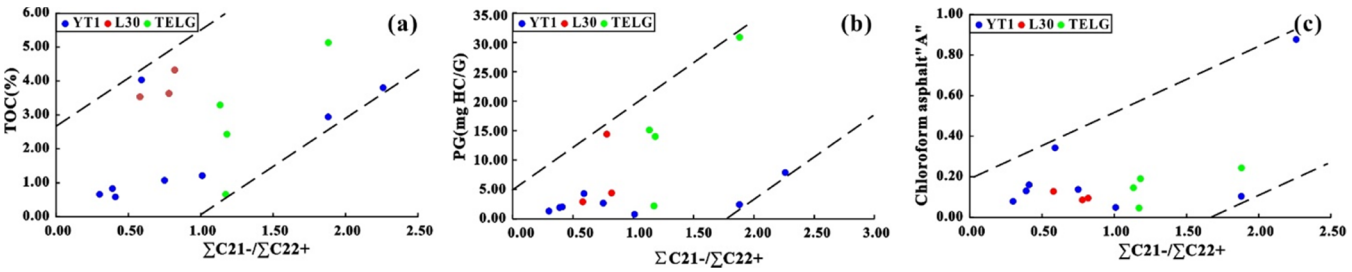

Figure 17. Relationship between $\sum C_{21-}/\sum C_{22+}$ and (a) TOC, (b) PG, and (c) chloroform asphalt A.

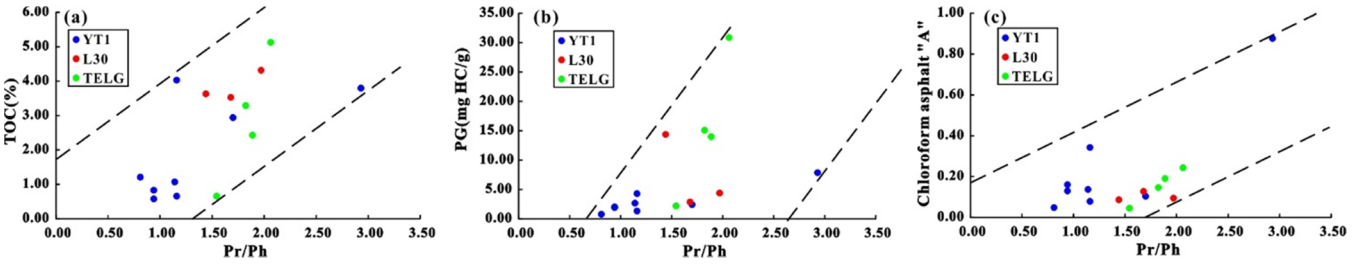

Figure 18. Relationship between Pr/Ph and (a) TOC, (b) PG,and (c) chloroform asphalt A.

which indicates that the warm and humid climate is conducive to the accumulation and preservation of organic matter, and the arid climate has an inhibitory effect on the occurrence of organic matter.

Previous studies[52−55] have found that the warm and humid paleoclimate environment is conducive to the survival and reproduction of aquatic organisms and terrestrial higher organisms, and it will also cause the water body to deepen and form a reducing environment, which is conducive to the preservation of organic matter. On the contrary, the arid paleoclimate is not conducive to the survival and reproduction of aquatic organisms, which leads to the decline of organic matter abundance. In addition, the paleoclimate has a certain control effect on the input of terrigenous detritus.[56] When the climate is humid, frequent precipitation makes a large number of provenance detritus fill, diluting the organic matter, which results in a less obvious relationship between the paleoclimate and organic matter abundance.

5.3.2. Influence of Organic Matter Input on Organic Matter Enrichment. The $\sum C_{21-}/\sum C_{22+}$ and TOC, PG and chloroform asphalt A are plotted (Figure 17). The results showed that the contents of TOC, PG, and chloroform asphalt A were weakly positively correlated with $\sum C_{21-}/\sum C_{22+}$, which indicated that aquatic organisms were conducive to the enrichment and preservation of organic matter, and the contribution of aquatic organisms to the occurrence of organic matter was greater than that of terrestrial higher plants.

The abundance of organic matter depends not only on the development of organisms but also on the input of organic matter. The input of organic matter mainly comes from various aquatic organisms and terrestrial higher plants. The former is the main contributor to organic matter abundance, while the latter provides nutrition for the former.[55,56]

5.3.3. Influence of Redox Environment on Organic Matter Enrichment. The relationship between Pr/Ph and TOC, PG, and chloroform asphalt A was drawn (Figure 18). The results showed that the values of TOC, PG, and chloroform asphalt A increased with the increase of the Pr/Ph value in the study area. The results are different from the previous understanding of "reducing environment for the conservation of organic matter". This shows that the oxidation−reduction environment has a certain control effect on the organic matter enrichment of Taodonggou group, but it is not the main control factor.

When the redox environment fluctuates, the abundance of organic matter changes greatly, and both redox environment and productivity will affect the preservation of organic matter.[32] Although the climate of Middle Permian in Taibei sag is semiarid and semihumid, the climate is mainly warm and humid.[36,57,58] Aquatic organisms and terrestrial higher organisms multiply in large numbers, forming high biological productivity. In addition, biological respiration can also increase oxygen consumption,[59,60] and high deposition rate can reduce the time of organic matter oxidation and decomposition,[60,61] which leads to the phenomenon of high concentration of organic matter in oxidation environment.

https://doi.org/10.1021/acsomega.1c04061
ACS Omega 2021, 6, 31578−31594

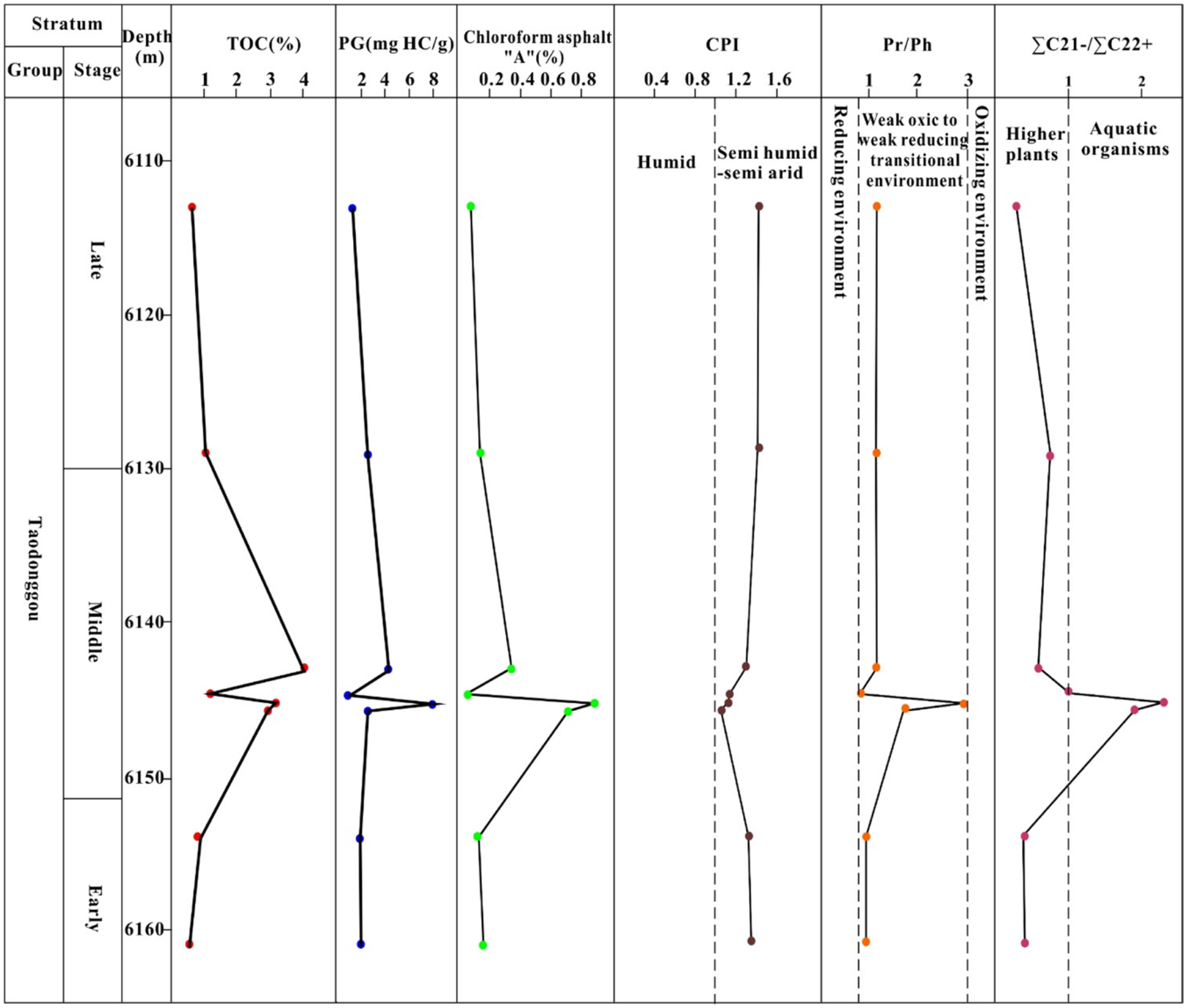

Figure 19. Vertical variation trend of TOC, PG, chloroform asphalt A, CPI, Pr/Ph, and $\sum C_{21-}/\sum C_{22+}$ in source rocks of Taodonggou group in the YT-1 well.

5.3.4. Enrichment Model of Organic Matter. Previous studies have found that the enrichment model of organic matter can be divided into three models: preservation model, productivity model, and productivity and anoxic interaction model.[62−65] Compared with the productivity model, the abundance of organic matter in Taodonggou group source rocks is higher in partial oxidation environment and lower in partial reduction environment. To further discuss the organic matter enrichment mechanism of Taodonggou group source rocks in Taibei sag, the Taodonggou group source rocks are divided into early, middle, and late stages (Figure 19).

In the early stage, the paleoclimate was dry with less precipitation, which resulted in less input of terrigenous detritus and nutrients, a slow reproduction rate of aquatic organisms, and low productivity. The input of organic matter was mainly terrigenous higher plants. Although the water body was a partial reducing environment, the low productivity made the organic matter abundance of the source rocks low (Figure 20a). In the middle stage, the paleoclimate gradually became warm and humid, which was conducive to the reproduction of terrestrial higher plants. In addition, precipitation accelerated the weathering of parent rocks, intensified the input of terrigenous detritus and nutrients, promoted the reproduction of aquatic organisms, and gave high biological productivity. Precipitation made the sedimentary water deeper, and the whole was in a partial oxidation environment, However, the high productivity makes the organic matter abundance of source rocks in this stage (Figure 20b). In the late stage, the paleoclimate became dry again and the productivity decreased, which resulted in the low abundance of organic matter in this stage. The above is the enrichment model of organic matter in Taodonggou group of Middle Permian in Taibei sag.

6. CONCLUSIONS

Based on the analysis of the organic petrology, organic geochemistry, sedimentary environment of the Middle Permian Taodonggou group source rocks, the influence factors on the enrichment of organic matter were revealed, and the enrichment model was established in the study area. The following conclusions can be obtained:

https://doi.org/10.1021/acsomega.1c04061
ACS Omega 2021, 6, 31578−31594

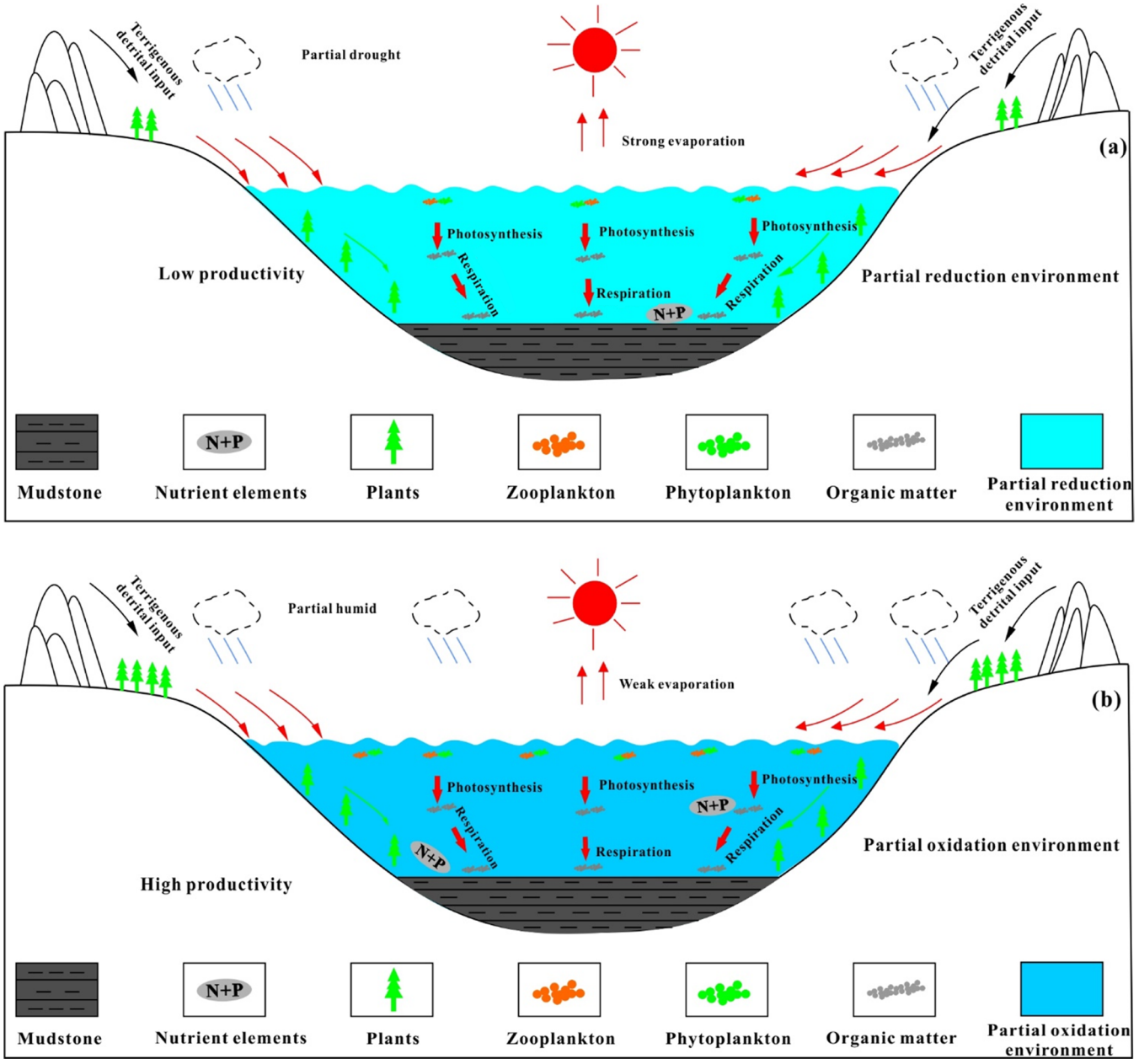

Figure 20. Enrichment model of organic matter in source rocks of Taodonggou group in Taibei sag: (a) early and late stage of Taodonggou group and (b) middle stage of Taodonggou group (modified after 62−65).

(1) The organic macerals of Taodonggou group source rocks in Taibei sag are mainly the exinite and sapropelite formation, followed by inertinite, and vitrinite is the least. The vitrinite mainly is vitrodetrinite, and the exinite is mainly lamalginiite.

(2) The source rocks of Taodonggou group in Taibei sag are mainly excellent source rocks. The types of organic matter are mainly type III and types II−III, which are in the mature stage, mainly in the oil window stage, and have a good hydrocarbon generation potential.

(3) The source rocks of Taodonggou group in Taibei sag were formed in a semihumid and semiarid climate with weak reduction and weak oxidation environments. The organic matter was transported into the mixed source. The terrestrial higher plants dominated in the early and late stage, and the aquatic organisms dominated in the middle stage. Under the coaction of paleoclimate, organic matter input, and redox environment, the enrichment model of organic matter with high productivity and weak oxidation environment characteristics can also form excellent source rocks.

AUTHOR INFORMATION

Corresponding Authors

Huan Miao − *School of Geoscience and Surveying Engineering, China University of Mining and Technology, Beijing 100083, China;* orcid.org/0000-0002-7958-3311; Email: 1627765379@qq.com

Jianying Guo − *Key Laboratory of Natural Gas Accumulation and Development, China National Petroleum Corporation, Langfang 065007, China*; Email: gjy_17711224@petrochina.com.cn

https://doi.org/10.1021/acsomega.1c04061
ACS Omega 2021, 6, 31578−31594

Authors

Yanbin Wang − *School of Geoscience and Surveying Engineering, China University of Mining and Technology, Beijing 100083, China*

Shihu Zhao − *School of Geoscience and Surveying Engineering, China University of Mining and Technology, Beijing 100083, China*

Xiaoming Ni − *School of Energy Science and Engineering, Henan Polytechnic University, Jiaozuo 454003, China*

Xun Gong − *School of Geoscience and Surveying Engineering, China University of Mining and Technology, Beijing 100083, China*

Yujian Zhang − *School of Geoscience and Surveying Engineering, China University of Mining and Technology, Beijing 100083, China*

Jianhong Li − *School of Geoscience and Surveying Engineering, China University of Mining and Technology, Beijing 100083, China*

Complete contact information is available at: https://pubs.acs.org/10.1021/acsomega.1c04061

Notes

The authors declare no competing financial interest.

■ ACKNOWLEDGMENTS

This study was supported by the Major National Science and Technology Project of China (grant nos. 2016ZX05066001-002, 2017ZX05064-003-001, and 2016zx05007) and the Science and Technology Projects of PetroChina (grant nos. 2019b-0601, 2019b-0602). The authors thank Key Laboratory of Natural Gas Accumulation, China, National Petroleum Corporation and Development and Turpan-Hami Oil Co. of CNPC for providing testing samples, and our colleagues for the beneficial suggestion.

■ REFERENCES

(1) Zhu, X. M.; Zhong, D. K.; Yuan, X. J.; Zhang, H. L.; Zhu, S. F.; Sun, H. T.; Gao, Z. Y.; Xian, B. Z. Development of sedimentary geology of petroliferous basins in China. *Pet. Explor. Dev.* **2016**, *43*, 890−901.

(2) Xu, C. C.; Zou, W. H.; Yang, Y. M.; Duan, Y.; Shen, Y.; Luo, B.; Ni, C.; Fu, X. D.; Zhang, J. Y. Status and prospects of deep oil and gas resources exploration and development onshore China. *J. Nat. Gas Geosci.* **2018**, *3*, 11−24.

(3) Li, J. Z.; Tao, X. W.; Bai, B.; Huang, S. P.; Jiang, Q. C.; Zhao, Z. Y.; Chen, Y. Y.; Ma, D. B.; Zhang, L. P.; Li, N. X.; Song, W. Geological conditions, reservoir evolution and favorable exploration directions of marine ultra-deep oil and gas in China. *Pet. Explor. Dev.* **2021**, *48*, 60−79.

(4) Guo, X. S.; Hu, D. F.; Li, Y. P.; Duan, J. B.; Zhang, X. F.; Fan, X. J.; Duan, H.; Li, W. C. Theoretical Progress and Key Technologies of Onshore Ultra-Deep Oil/Gas Exploration. *Engineering* **2019**, *5*, 458−470.

(5) Fan, D. L.; Li, F. B.; Wang, Z. L.; Miao, Q.; Bai, Y.; Liu, Q. Y. Development status and prospects of China's energy minerals under the target of carbon peak and carbon neutral. *Chin. Min. Mag.* **2021**, *30*, 1−8.

(6) Zou, C. N.; Zhu, R. K.; Chen, Z. Q.; Ogg, J. G.; Wu, S. T.; Dong, D. Z.; Qiu, Z.; Wang, Y. M.; Wang, L.; Lin, S. H.; Cui, J. W.; Su, L.; Yang, Z. Organic-matter-rich shales of China. *Earth-Sci. Rev.* **2019**, *189*, 51−78.

(7) Liang, S. J. Achievements and potential of petroleum exploration in tuha oil and gas province. *Xinjiang Pet. Geol.* **2020**, *41*, 631−641.

(8) Gang, G.; Hao, L.; Li, H. M.; Jiao, L. X.; Wang, Z. Y.; Hou, Q. Z. Organic geochemistry of Carboniferous and Lower Permian source rocks, Turpan-Hami Basin, NW China. *Pet. Explor. Dev.* **2009**, *36*, 583−592.

(9) Sun, M.; Gu, W. P.; Liu, Y.; Wang, D. R.; Yang, B. In *Deep Seismic Acquisition Technology and Application Effect of pre Jurassic in Turpan Hami Basin*, SPG/SEG Nanjing 2020 International Geophysical Conference 2020, Nanjing, China, 2020.

(10) Jiang, S. H.; Li, S. Z.; Somerville, I. D.; Lei, J. P.; Yang, H. Y. Carboniferous−Permian tectonic evolution and sedimentation of the Turpan-Hami Basin, NW China: Implications for the closure of the Paleo-Asian Ocean. *J. Asian Earth Sci.* **2015**, *113*, 644−655.

(11) Wali, G.; Wang, B.; Cluzel, D.; Zhong, L. L. Carboniferous − Early Permian magmatic evolution of the Bogda Range (Xinjiang, NW China): Implications for the Late Paleozoic accretionary tectonics of the SW Central Asian Orogenic Belt. *J. Asian Earth Sci.* **2018**, *153*, 238−251.

(12) Shi, Y. Q.; Ji, H. C.; Yu, J. W.; Xiang, P. F.; Yang, Z. B.; Liu, D. D. Provenance and sedimentary evolution from the Middle Permian to Early Triassic around the Bogda Mountain, NW China: A tectonic inversion responding to the consolidation of Pangea. *Mar. Pet. Geol.* **2020**, *114*, No. 104169.

(13) Li, X. Q.; Zhong, N. N.; Xiong, B.; Wang, T. G. Application of whole rock analysis in source rock research and comparison with kerogen analysis. *Pet. Explor. Dev.* **1995**, *22*, 30−40.

(14) Powell, T. G.; Mckirdy, D. M. Relationship between ratio of pristane to phytane, crude oil composition and geological environment in Australia. *Nat. Phys. Sci.* **1973**, *243*, 37−39.

(15) Peters, K. E.; Molodowan, J. M. *The Biomarker Guide: Interpreting Molecular Fossils in Petroleum and Ancient Sediments*; Prentice Hall: New Jersey, 1993.

(16) Moldowan, J. M.; Sundararaman, P.; Schoell, M. Sensitivity of biomarker properties to depositional environment and/or source input in the Lower Toarcian of SW-Germany. *Org. Geochem.* **1986**, *10*, 915−926.

(17) Damsté, J. S. S.; Kenig, F.; Koopmans, M. P.; Köster, J.; Schouten, S.; Hayes, J. M.; Leeuw, J. W. Evidence for gammacerane as an indicator of water column stratification. *Geochim. Cosmochim. Acta* **1995**, *59*, 1895−1900.

(18) Peters, K. E.; Moldowan, J. M.; Sundararaman, P. Effects of hydrous pyrolysis on biomarker thermal maturity parameters: Monterey Phosphatic and Siliceous members. *Org. Geochem.* **1990**, *15*, 249−265.

(19) Xu, X. F.; Xu, S. H.; Liu, J.; Chen, L.; Liang, H. R.; Mei, L. F.; Liu, Z. Q.; Shi, W. Z. Thermal maturation, hydrocarbon generation and expulsion modeling of the source rocks in the Baiyun Sag, Pearl River Mouth Basin, South China Sea. *J. Pet. Sci. Eng.* **2021**, *205*, No. 108781.

(20) Chen, J. P.; Zhao, C. Y.; He, Z. H. Discussion on evaluation criteria for hydrocarbon generation potential of organic matter in coal measures. *Pet. Explor. Dev.* **1997**, *24*, 1−5.

(21) Tissot, B. P.; Welte, D. H. *Petroleum Formation and Occurrence: A New Approach to Oil and Gas Exploration*; Springer-Verlag, 1978.

(22) Makeen, Y. M.; Abdullah, W. H.; Hakimi, M. H.; Mustapha, K. A. Source rock characteristics of the Lower Cretaceous Abu Gabra Formation in the Muglad Basin, Sudan, and its relevance to oil generation studies. *Mar. Pet. Geol.* **2015**, *59*, 505−516.

(23) Ahmed, N.; Siddiqui, N. A.; Rahman, A. H. B. A.; Jamil, M.; Usman, M.; Sajid, Z.; Zaidi, F. K. Evaluation of hydrocarbon source rock potential: Deep marine shales of Belaga Formation of Late Cretaceous-Late Eocene, Sarawak, Malaysia. *J. King Saud Univ., Sci.* **2021**, *33*, No. 101268.

(24) Mani, D.; Patil, D. J.; Dayal, A. M.; Prasad, B. N. Thermal maturity, source rock potential and kinetics of hydrocarbon generation in Permian shales from the Damodar Valley basin, Eastern India. *Mar. Pet. Geol.* **2015**, *66*, 1056−1072.

(25) Goodarzi, F.; Haeri-Ardakani, O.; Gentzis, T.; Pedersen, P. K. Organic petrology and geochemistry of Tournaisian-age Albert Formation oil shales, New Brunswick, Canada. *Int. J. Coal Geol.* **2019**, *205*, 43−57.

(26) Khan, I.; Zhong, N. N.; Luo, Q. Y.; Ai, J. Y.; Yao, L. P.; Luo, P. Maceral composition and origin of organic matter input in Neoproterozoic−Lower Cambrian organic-rich shales of Salt Range Formation, upper Indus Basin, Pakistan. *Int. J. Coal Geol.* **2020**, *217*, No. 103319.
(27) Cao, Q. Y. Identification of microcomponents and types of kerogen under transmitted light. *Pet. Explor. Dev.* **1985**, *12*, 14−23.
(28) Gao, J. L.; Ni, Y. Y.; Li, W.; Yuan, Y. L. Pyrolysis of coal measure source rocks at highly to over mature stage and its geological implications. *Pet. Explor. Dev.* **2020**, *47*, 773−780.
(29) Kumar, S.; Das, S.; Bastia, R.; Ojha, K. Mineralogical and morphological characterization of Older Cambay Shale from North Cambay Basin, India: Implication for shale oil/gas development. *Mar. Pet. Geol.* **2018**, *97*, 339−354.
(30) Radke, M.; Welte, D. H.; Willsch, H. Maturity parameters based on aromatic hydrocarbons: Influence of the organic matter type. *Org. Geochem.* **1986**, *10*, 51−63.
(31) Liu, B.; Liang, D.; Jie, F.; Jia, R.; Fu, J. Organic Matter Maturity and Oil/Gas Prospects in Middle-Upper Proterozoic and Lower Paleozoic Carbonate Rocks in Northern China. *Chin. J. Geochem.* **1986**, *5*, 55−70.
(32) Wu, W.; Liu, W. Q.; Mou, C. L.; Liu, H.; Qiao, Y.; Pan, J. N.; Ning, S. Y.; Zhang, X. X.; Yao, J. X.; Liu, J. D. Organic-rich siliceous rocks in the upper Permian Dalong Formation (NW middle Yangtze): Provenance, paleoclimate and paleoenvironment. *Mar. Pet. Geol.* **2021**, *123*, No. 104728.
(33) Li, C. L.; Ma, S. P.; Xia, Y. Q.; He, X. B.; Gao, W. Q.; Zhang, G. Q. Assessment of the relationship between ACL/CPI values of long chain n-alkanes and climate for the application of paleoclimate over the Tibetan Plateau. *Quat. Int.* **2020**, *544*, 76−87.
(34) Xu, J. Y.; Niu, Y. B.; Xu, S. K.; Zhao, X. W. Main controlling factors and development model of the Miocene marine source rocks in Yinggehai basin. *Bull. Geol. Sci. Technol.* **2021**, *40*, 54−63.
(35) Luo, P.; Peng, P. G.; Lü, H.; Zheng, Z.; Wang, X. Latitudinal variations of CPI values of long-chain n-alkanes in surface soils: Evidence for CPI as a proxy of aridity. *Sci. China: Earth Sci.* **2012**, *55*, 1134−1146.
(36) Wei, X. X.; Zhang, X. H.; Huang, X.; Luan, T. F. Palaeoclimate reconstruction of Middle Permian in Tuha basin: evidence from the fossil wood growth rings. *Earth Sci.* **2016**, *41*, 1771−1780.
(37) Bohacs, K. M.; Grabowski, G. J., Jr.; Carroll, A. R.; Mankiewicz, P. J. Production, Destruction, and Dilution—The Many Paths to Source-Rock Development 2005, *82*, 61 101.
(38) Huang, B. C.; Zhou, Y. X.; Zhu, R. X. Discussions on Phanerozoic evolution and formation of continental China, based on paleomagnetic studies. *Earth Sci. Front.* **2008**, *15*, 348−359.
(39) Requejo, A. G.; Hieshima, G. B.; Hsu, C. S.; McDonald, T. J.; Sassen, R. Short-chain (C21 and C22) diasteranes in petroleum and source rocks as indicators of maturity and depositional environment. *Geochim. Cosmochim. Acta.* **1997**, *61*, 2653−2667.
(40) Tan, Z. Z.; Lu, S. F.; Li, W. H.; Zhang, Y. Y.; He, T. H.; Jia, W. L.; Peng, P. A. Climate-driven variations in the depositional environment and organic matter accumulation of lacustrine mudstones: Evidence from organic and inorganic geochemistry in the Biyang Depression, Nanxiang Basin. China. *Energy Fuels* **2019**, *33*, 6946−6960.
(41) Sachsenhofer, R. F.; Popov, S. V.; Akhmetiev, M. A.; Bechtel, A.; Gratzer, R.; Gross, D.; Horsfield, B.; Rachetti, A.; Rupprent, B.; Schaffar, W. B. H.; et al. The type section of the Maikop Group (Oligocene-Lower Miocene) at the Belaya River (North Caucasus): depositional environment and hydrocarbon potential. *AAPG Bull.* **2017**, *101*, 289−319.
(42) Seifert, W. K.; Moldowan, J. M. Use of biological makers in petroleum exploration. *Methods Geochem. Geophys.* **1986**, *24*, 261−290.
(43) Gelpi, E.; Schneider, H.; Mann, J.; Oró. Hydrocarbons of geochemical significance in microscopic algae. *Phytochemistry* **1970**, *9*, 603−612.
(44) Huang, W. Y.; Meinschein, W. G. Sterols as ecological indicators. *Geochim. Cosmochim. Acta* **1979**, *43*, 739−745.
(45) Connan, J.; Cassou, A. M. Properties of gases and petroleum liquids derived from terrestrial kerogen at various maturation levels. *Geochim. Cosmochim. Acta* **1980**, *44*, 1−23.
(46) Bohacs, K. M.; Grawbowski, G. J.; Carroll, A. R.; Mankeiwitz, P. J.; Miskell-Gerhardt, K. J.; Schwalbach, J. R.; Wegner, M. B.; Simo, J. A. Production, destruction, and dilution-the many paths to source-rock development. *SEPM Spec. Publ.* **2005**, *82*, 61−101.
(47) Adams, D.; Hurtgen, M.; Sageman, B. Volcanic triggering of a biogeochemical cascade during Oceanic Anoxic Event 2. *Nat. Geosci.* **2010**, *3*, 201−204.
(48) Ji, W. M.; Hao, F.; Song, Y.; Tian, J. Q.; Meng, M. M.; Huang, H. X. Organic geochemical and mineralogical characterization of the lower Silurian Longmaxi shale in the southeastern Chongqing area of China:Implications for organic matter accumulation. *Int J. Coal Geol.* **2020**, *220*, No. 103412.
(49) Xu, H.; Xie, Q. L.; Wang, S. M.; Yu, S. Organic geochemical characteristics and gas prospectivity of Permian source rocks in western margin of Songliao Basin, northeastern China. *J. Pet. Sci. Eng.* **2021**, *205*, No. 108863.
(50) Passey, Q. R.; Bohacs, K.; Esch, W. L.; Klimentidis, R.; Sinha, S. In *From Oil-Prone Source Rock to Gas-Producing Shale Reservoir - Geologic and Petrophysical Characterization of Unconventional Shale Gas Reservoirs*, SPE-131350, CPS/SPE International Oil & Gas Conference and Exhibition in China, Beijing, China., 2010.
(51) Hu, T.; Pang, X. Q.; Jiang, S.; Wang, Q. F.; Xu, T. W.; Lu, K.; Huang, C.; Chen, Y. Y.; Zheng, X. W. Impact of Paleosalinity, Dilution, Redox, and Paleoproductivity on Organic Matter Enrichment in a Saline Lacustrine Rift Basin: A Case Study of Paleogene Organic-Rich Shale in Dongpu Depression, Bohai Bay Basin, Eastern China. *Energy Fuels* **2018**, *32*, 5045−5061.
(52) Liang, H. R.; Xu, G. S.; Xu, F. H.; Yu, Q.; Liang, J. J.; Wang, D. Y. Paleoenvironmental evolution and organic matter accumulation in an oxygen-enriched lacustrine basin: A case study from the Laizhou Bay Sag, southern Bohai Sea (China). *Int. J. Coal Geol.* **2019**, *217*, No. 103318.
(53) Fang, Z.; Pu, X. G.; Chen, S. R.; Yan, J. H.; Han, W. Z.; Shi, Z. N.; Zhang, W.; Chen, X. R.; Dong, Q. M. Investigation of enrichment characteristic of organic matter in shale of the 2nd member of Kongdian formation in Cangdong sag. *J. Chin. Univ. Min. Technol.* **2021**, *50*, 304−317.
(54) Ma, Y. Q.; Fan, M. S.; Lu, Y. C.; Liu, H. M.; Hao, Y. Q.; Xie, Z. H.; Liu, Z. H.; Peng, L.; Du, X. B.; Hu, H. Y. Climate-driven paleolimnological change controls lacustrine mudstone depositional process and organic matter accumulation: Constraints from lithofacies and geochemical studies in the Zhanhua Depression, eastern China. *Int. J. Coal Geol.* **2016**, *167*, 103−118.
(55) Yang, W. Q.; Wang, X. J.; Jiang, Y. L.; Zhang, S.; Wang, Y.; Zhu, D. Y.; Zhu, D. S. Quantitative reconstruction of paleoclimate and its effects on fine-grained lacustrine sediments:A case study of the upper Es4 and lower Es3 in Dongying Sag. *Pet. Geol. Recovery Effic.* **2018**, *25*, 29−36.
(56) Cichon-Pupienis, A.; Littke, R.; Lazauskienė, J.; Baniasad, A.; Pupienis, D.; Radzevičius, S.; Šiliauskas, L. Geochemical and sedimentary facies study − Implication for driving mechanisms of organic matter enrichment in the lower Silurian fine-grained mudstones in the Baltic Basin (W Lithuania). *Int. J. Coal Geol.* **2021**, *244*, No. 103815.
(57) Liu, L. J.; Yao, Z. Q. Early Late Permian Flora from Turpan Hami Basin. *Acta Palaeontol. Sin.* **1996**, *35*, 644−677.
(58) Wu, S. Z. Paleoclimate of lower Permian in Xinjiang. *Xinjiang Geol.* **1996**, *14*, 270−277.
(59) Soares, A.; Berggren, M. Indirect link between riverine dissolved organic matter and bacterioplankton respiration in a boreal estuary. *Mar. Environ. Res.* **2019**, *148*, 39−45.
(60) Ding, J. H.; Zhang, J. C.; Shi, G.; Shen, B. J.; Tang, X.; Yang, Z. Z.; Li, X. Q.; Li, C. X. Sedimentary environment and organic matter enrichment mechanisms of the Upper Permian Dalong Formation

https://doi.org/10.1021/acsomega.1c04061
ACS Omega 2021, 6, 31578−31594

shale,southern Anhui Province, China. *Oil Gas Geol.* **2021**, *42*, 158−172.
(61) Xue, J.; Liu, L. F.; Sun, H. F.; Huang, S. B.; Geng, M.; Chen, Y.; Li, S. P.; Shen, N. Differential distributin of high-qualiity lacustrine source rocks controlled by climate and tectonics: a case study from Bozhong sag. *Acta Pet. Sin.* **2019**, *40*, 165−175.
(62) Calvert, S. E.; Fontugne, M. R. On the Late Pleistocene - Holocene Sapropel Record of Climatic and Oceanographic Variability in the Eastern Mediter - ranean. *Paleoceanography* **2001**, *16*, 78−94.
(63) Sageman, B. B.; Murphy, A. E.; Werne, J. P.; Straten, C. A. V.; Hollander, D. J.; Lyons, T. W. A Tale of Shales: The Relative Roles of Production, Decomposition, and Dilution in the Accumulation of Organic-Rich Strata, Middle− Upper Devonian, Appa-lachian Basin. *Chem. Geol.* **2003**, *195*, 229−273.
(64) Mort, H.; Jacquat, O.; Adatte, T.; Steinmann, P.; F?Llmi, K.; Matera, V.; Berner, Z.; Stüben, D. The Cenomanian/Turonian Anoxic Event at the Bonarelli Level in Italy and Spain: Enhanced Productivity and/or Better Preservation? *Cretaceous Res.* **2007**, *28*, 597−612.
(65) Li, W. H.; Lu, S. F.; Tan, Z. Z.; Taohua He, T. H. Lacustrine Source Rock Deposition in Response to Coevolution of the Paleoenvironment and Formation Mechanism of Organic-Rich Shales in the Biyang Depression, Nanxiang Basin. *Energy Fuels* **2017**, *31*, 13519−13527.

https://doi.org/10.1021/acsomega.1c04061
ACS Omega 2021, 6, 31578−31594